Heliyon 10 (2024) e28355

Contents lists available at ScienceDirect

Heliyon

journal homepage: www.cell.com/heliyon

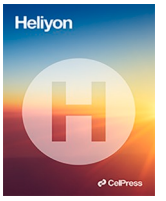

Research article

Reliable differentiation of necrosis and active metabolically contours of glioblastoma multiforme using susceptibility-based imaging

Anita Ebrahimpour [a,*], Mehdi Khoobi [b], Nader Riyahi Alam [a], Mahboubeh Masoumbeigi [c], Fatemeh Tirgar [d], Tayyebeh Ebrahimi [a]

[a] Department of Medical Physics and Biomedical Engineering, Faculty of Medicine, Tehran University of Medical Sciences, Tehran, Iran
[b] Department of Medicinal Chemistry, Faculty of Pharmacy, Tehran University of Medical Sciences, Tehran, Iran
[c] Department of Radiology, Faculty of Para-Medicine, Hormozgan University of Medical Sciences, Bandar Abbas, Iran
[d] Department of Neuroscience and Addiction Studies, School of Advanced Technologies in Medicine, Tehran University of Medical Sciences, Tehran, Iran

ARTICLE INFO

Keywords:
Glioblastoma multiforme
Gadolinium-enhancing necrosis
Active metabolically contours
5-Aminolevulinic acid
Quantitative susceptibility mapping

ABSTRACT

Purpose: Gadolinium-enhancing necrosis in glioblastoma multiforme (GBM), as an occasionally occurring false positive in contrast enhancement (CE) imaging, leads to trouble for segmentation of GBM and treatment. Therefore, the investigation of complementary detection way to identify the metabolically active volume of the tumor with high reliability is very worth to be addressed. Here, we reported on a case of GBM with gadolinium-enhancing necrosis in an experimental CE imaging study in mice and evaluated the discrimination of the necrosis and metabolically active parts of the GBM using conventional and state-of-the-art susceptibility-based MRI.

Methods: In this study, following 5-aminolevulinic acid (ALA) and iron supplements (FAC, 6 h after ALA, intra-tumoral injection) to animal, T_2*-W imaging and quantitative susceptibility mapping (QSM) were performed, and compared with CE imaging.

Results: The signal intensity (SI) of the active and necrosis areas of the case in the CE image demonstrated no significant difference while the SI on the T_2*-W images and susceptibility value in QSM changed 24 and 150%, respectively.

Conclusion: The preclinical case report provides valuable insights into the potential of susceptibility-based MRI using ALA + FAC to apply as a robust discriminator between necrotic and viable tumors.

1. Introduction

Glioblastoma Multiforme (GBM) is a malignant type of brain tumor and featured with a high recurrence rate and poor diagnosis [1]. Therefore, Recent studies have addressed the development of effective imaging techniques achieving the accurate segmentation of tumor [2]. Magnetic resonance imaging (MRI) using contrast enhancement (CE) based on gadolinium is the common method of choice for the evaluation of GBM [3]. However, this method has inherent obstacles, such as Gd-related toxicity [4,5] and a poor detection of active parts of the tumor [6,7] causing enhancement of necrosis area (false positive) in some cases [8]. Gadolinium-enhancing necrosis

* Corresponding author.
E-mail addresses: anitaebrahimpor@gmail.com, a-ebrahimpour@tums.ac.ir (A. Ebrahimpour).

https://doi.org/10.1016/j.heliyon.2024.e28355
Received 27 September 2023; Received in revised form 16 March 2024; Accepted 17 March 2024
Available online 24 March 2024

could be mistaken for active tumor, leads to Gadolinium-enhancing necrosis in glioblastoma multiforme (GBM), as an occasionally occurring false positive in contrast enhancement (CE) imaging, leads to trouble for segmentation of GBM and treatment. Therefore, new imaging technique for detecting active volumes of the tumor with high sensitivity and specificity is very worth to be addressed.

Therefore, recent studies focused on fluorescence imaging (FI) of brain tumor with 5-aminolevulinic acid (ALA) as a useful way to visualize the active parts of GBM with fluorescent ALA-induced protoporphyrin IX (PpIX) accumulation, intraoperatively [9–11]. However, there are some pitfalls in this method, including dependency of the fluorescence intensity to the distance and direction of the light source, photobleaching, absorption of the light source with hemorrhages, and leakage of PpIX [10].

In 2014, Cho et al. first demonstrated the applicability of ALA in MR imaging for the detection of malignant glioma using a 7 T scanner in an animal model [12]. The study revealed that dosage of 100 mg/kg ALA caused the accumulation of iron in GBM creating T2*-W (T2*-W) contrast in tumor areas.

Recently, we conducted an experimental imaging study to introduce "ALA with standard dosage (20 mg/kg) plus iron supplement (ferric ammonium citrate (FAC))" as an effective agent for creating augmented ferritin clusters in high-grade glioma representing clinical MRI (3 T) contrast due to its susceptibility effect [13]. As a piece of supportive information, the accumulation of ferritin clusters has been demonstrated on tumor sections of an animal after administration of "ALA + FAC" using Prussian blue staining (Fig. 1 (a–d)).

However, the specificity of this method still remains unclear. Therefore, in the current study, the effectiveness of this metabolic method for truly discriminative detection between necrosis and active volumes of GBM was demonstrated using T_2*-W magnitude and QSM in comparison with other methods, including CE, and FI.

2. Materials and methods

2.1. Animal imaging

First, a total of 1.5×10^6 C_6 glioma cells were injected into the right frontal lobe of rat brain. After two weeks, six male C_6 rat GBM model (weighing 220–250 g, 6–8 weeks, Iranian Pasteur Institute, Tehran, Iran) received ALA (25 mg/kg, subcutaneous injections) and/or of FAC (1 mM, 4 μL, 6 h after ALA, intra-tumoral injection), and the detection of GBM was evaluated using T_2* and QSM (6). Also, each animal received dotarem (Gd-DOTA), and was imaged using CE imaging [14].

The case animal was randomized to the "ALA + FAC" group. After administration of ALA and FAC, MR imaging was performed using a MRI scanner (3T, Siemens Prisma, Erlangen, Germany) with a 2-channel phased-array coil for rat brain using a 3D T_2*-W gradient-echo sequence [14]. Furthermore, for the T_1-W magnitude images, a 2D T_1-W turbo spin-echo sequence was used after administration of Dotarem (Guerbet, France; 0.1 mmol/kg body weight). All parameters of imaging were set as our previous study [13].

To verify the active parts of the GBM using FI, rat-bearing GBM was also injected with 100 mg/kg of ALA intraperitoneally. Six hours later, brain sections of a rat imaged using a small animal in vivo optical imaging system (Excitation: 430 nm, Emission: 600–700 nm, Fluovision, Iran).

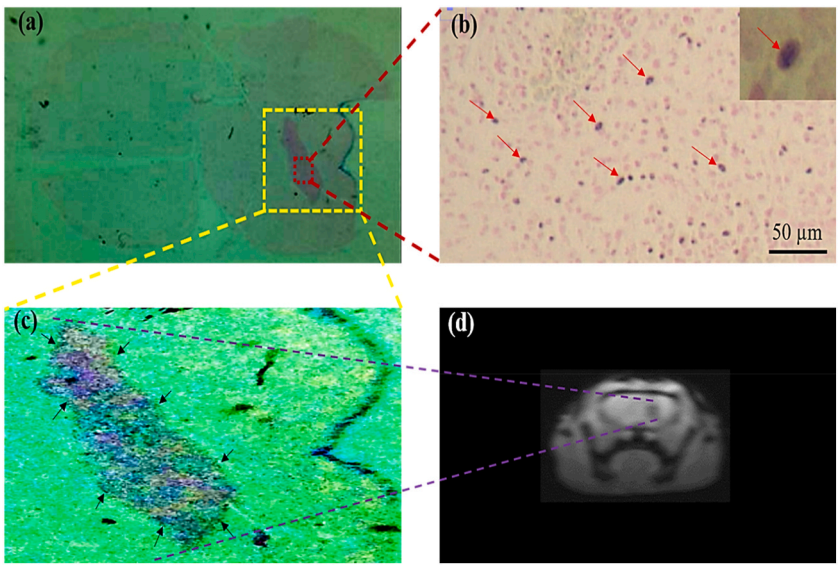

Fig. 1. (a–c) Prussian blue staining of a section of rat brain containing GBM after administration of 'ALA + FAC'. (b) Red arrows demonstrate ferritin clusters in the cytoplasm of tumor cells with a size of more than 1 μm (d) Corresponding T_2*-W magnitude image with clear signal loss in tumor area accumulated with ferritins. Based on the stained GBM images, a specific accumulation of ferritin clusters in the tumor cells was verified. (For interpretation of the references to colour in this figure legend, the reader is referred to the Web version of this article.)

2.2. Quantitative analysis

The estimation of susceptibility values of GBM was performed with the QSM algorithm using T_2*-W phase and magnitude images as described in the previous study [14] and summarized in Fig. 2. Briefly, the rat brain images were masked in MIPAV software. Then, phase unwrapping and background field removal were conducted using Laplacian-based algorithm and PDF algorithm, respectively. Finally, the estimation of magnetic susceptibility was performed with the MEDI method using Matlab software [31].

The histograms and mean SI of three regions of the brain (active area of GBM, necrosis area of GBM, and non-tumor brain tissue) were obtained for T_2*-W images, susceptibility map, post-contract T_1-W images, and also fluorescence images using ALA (Fig. 2).

2.3. Statistical analysis

For statistical analysis between three regions of the brain (active area of GBM, necrosis area of GBM, and non-tumor brain tissue), analysis of variance (ANOVA) was used for all quantitative parameters. The software used for this study was Prism 8 (version 8.0.2, GraphPad Software, San Diego, Calif) and Matlab (the Mathwork, Inc., Natick, Ma, USA) for statistical analysis (significance level of less than 0.05).

3. Results

2D histogram of necrosis areas of the tumor had a distribution of pixels with higher intensity than the active parts of the tumor on the T_1-W image after administration of dotarem. In the necrosis area, an enhancement was observed, representing a case of gadolinium-enhancing necrosis (Fig. 3d). However, there was no significant difference between the active and necrosis areas (153 ± 6 vs. 149 ± 8 a. u., $P > 0.05$, Fig. 3(a–c)).

However, 2D histograms of the active parts of the tumor revealed a distribution of pixels with lower intensity for the T_2*-W image and higher intensity for the susceptibility map than the necrosis area after administration of "ALA + FAC" (153 ± 8 vs. 117 ± 7 a. u. for T_2*-W image, Fig. 4(a–d) and 0.4 ± 0.2 vs. -0.8 ± 0.7 ppm for susceptibility, $p < 0.05$, Fig. 4(e–j)). No enhancement was found in the necrosis part for the QSM (Fig. 4h).

There was a distribution of pixels with higher fluorescence intensity for the active part of the GBM than the necrosis (252 ± 5 vs. 208 ± 8 a. u., $P < 0.05$, Fig. 5(a–c)). A clear enhancement was seen in the active regions of the GBM in the ALA-based fluorescence image Fig. 5(d), which was consistent with the enhanced area in QSM.

4. Discussion

In this study we present a metabolic imaging approach to allow highly accurate discrimination of the necrosis and metabolically active areas of the GBM in an animal case using susceptibility-based MRI and compared with the conventional method.

Over the last several years, the fluorescence property of ALA has been utilized as a neurosurgical adjunct to aid the discrimination of tumor and normal brain, which has been widely documented in the literature [15–17]. In 2014, ALA (dosage of 100 mg/kg) was reported for the first time as an MRI contrast agent creating T_2*-based contrast using a 7 T scanner, which was not clinically applicable [12]. To make ALA in MRI clinical applicable, we previously introduced "ALA plus iron" as a metabolic method to detect GBM with

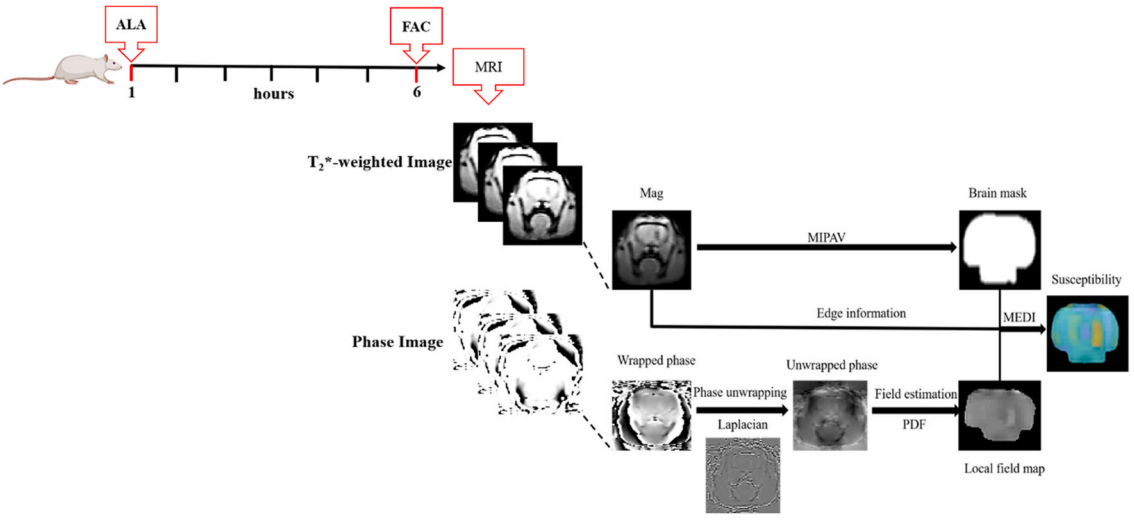

Fig. 2. Overview of the study protocol and QSM pipeline, including brain mask, phase unwrapping using the laplacian method, local field map using projection onto dipole fields (PDF), and susceptibility estimation with morphology enabled dipole inversion (MEDI) algorithm.

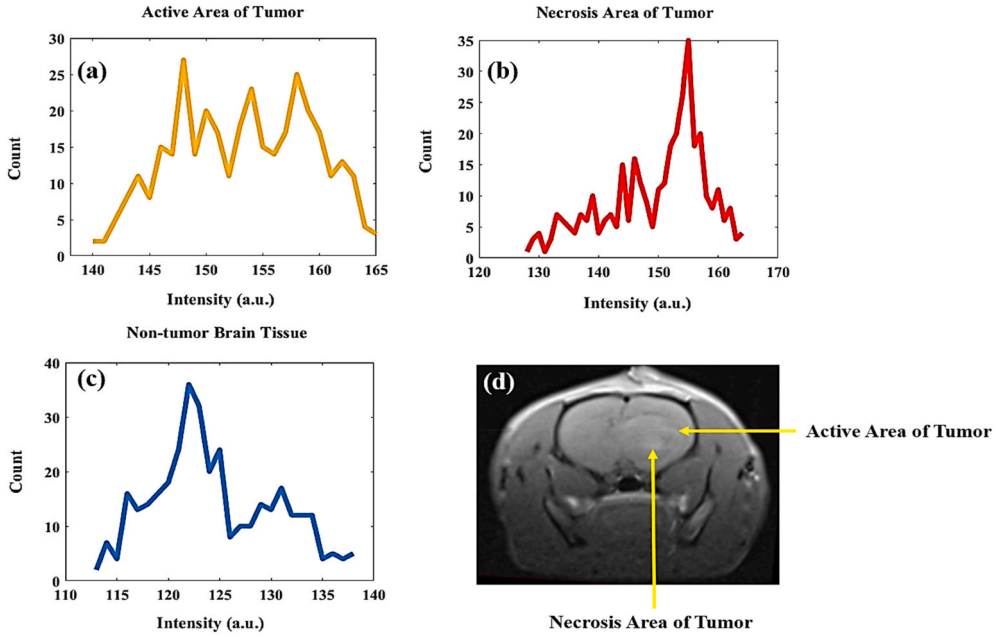

Fig. 3. 2D histograms of the (a) active area of the tumor, (b) necrosis area of the tumor, and (c) non-tumor brain tissue after administration of dotarem for T_1-W contrast enhancement (CE) image in MRI. (d) The corresponding MR image was also shown. A clear enhancement was seen in the necrosis part compared with the active area of the tumor (false positive).

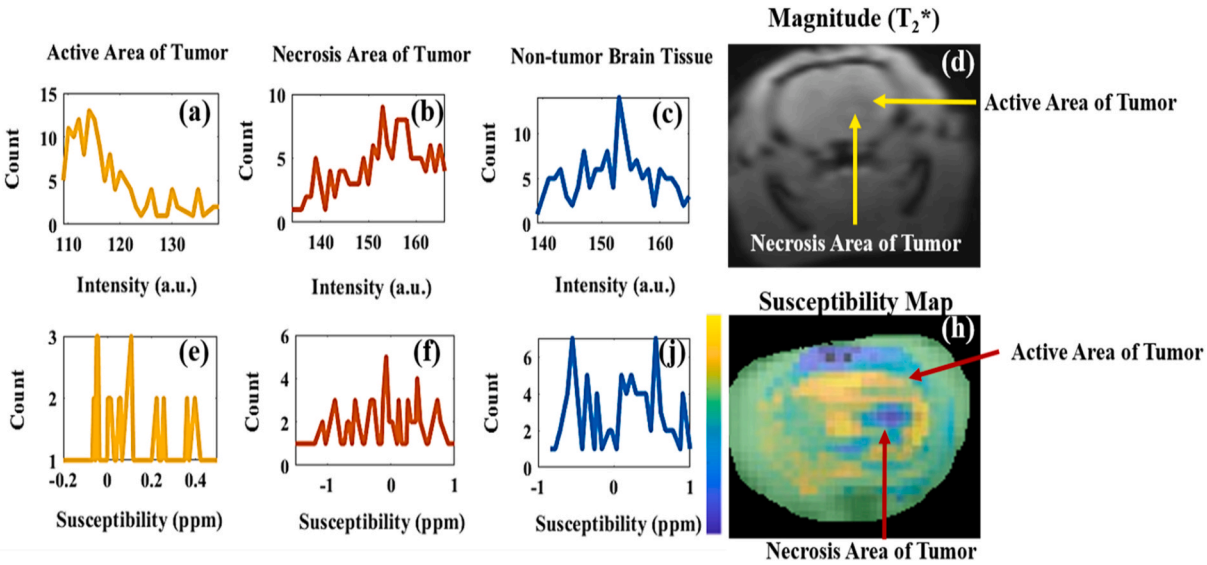

Fig. 4. 2D histograms of the active part of the tumor, necrosis area of the tumor, and non-tumor brain tissue after administration of "ALA + FAC" for (a–c) T_2*-W image (e–j) and QSM. Corresponding images or map were shown in the first right column. There was a significant contrast between necrosis and the active part of the GBM. No enhancement was found in the necrosis part in QSM (true negative).

high sensitivity using the standard dosage of ALA (20 mg/kg) and a clinical 3 T scanner [13]. However, in the current work, we focused on the ability of "ALA plus iron" as a metabolic method in susceptibility-based MRI to discriminate the necrosis and metabolically active areas of the tumor, in comparison to T_1-W CE.

In the T_1-W image, a clear enhancement was seen in the necrosis part (False Positive), representing possible penetration of contrast into the necrotic area [8]. While in the same case, non-enhancing necrotic area and enhancing viable tumor were discriminately observed using fluorescence imaging, after ALA, and susceptibility-based MRI, after "ALA + FAC", due to more activation of the heme signaling pathway in mitochondria by ALA and iron creating augmented fluorescent protoporphyrin IX (PpIX) and superparamagnetic ferritin clusters in viable cells as reliable metabolic biomarkers [13,18].

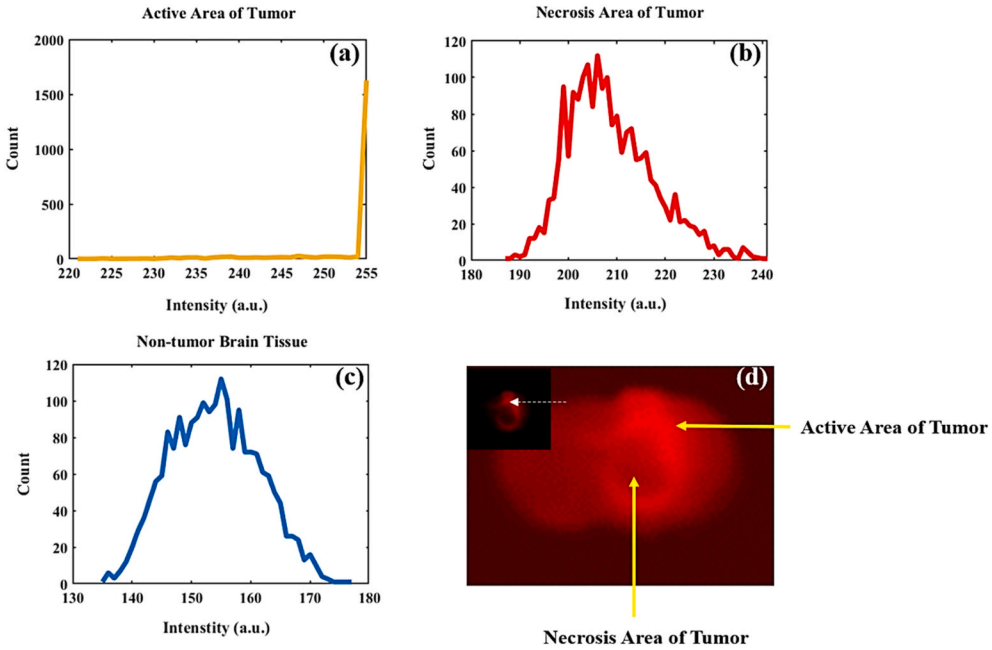

Fig. 5. 2D histograms of the (a) active area of the tumor, (b) necrosis area of the tumor, and (c) non-tumor brain tissue after administration of ALA for fluorescence image. (d) The corresponding fluorescence image was also shown. A clear enhancement was seen in the active areas of the GBM in the ALA-based fluorescence image (true negative).

Superparamagnetic ferritin clusters create magnetic field inhomogeneity leading to the proton spin dephasing and darkening of T_2*-W images with a physical mechanism called static dephasing regime (SDR) or slow-motion regime [19]. There are some reasons for considering SDR; the first one is to identify no change of signal intensity in the T_2-W image after "ALA + FAC" (supplementary data), despite a significant decrease of signal intensity in T_2*-W images [14]. This reveals the complete elimination of spin dephasing induced by field inhomogeneity using a 180° radiofrequency pulse in a spin-echo sequence, representing a lack of spin dephasing caused by diffusion called motion-narrowing regime [20]. The second one is forming ferritin clusters with a size of more than 1 μm, as shown with the Prussian blue staining of the GBM. It has been proved that SDR can be considered as physical model in MRI for ferritin clusters having a size of about 0.4 μm or more in the brain for a 3T scanner [21]. Therefore, it could be concluded that field inhomogeneity is the main susceptibility effect of ferritin clusters, which has a linear relationship with phase changes in gradient-echo images. By deconvolving the phase information to map ferritin distribution as the susceptibility source, QSM opens the door to study viable tumor without blooming artifact [22,23].

Interestingly, the current study reveals that QSM followed by ALA + FAC illuminates a promising potential to apply as a robust discriminator between necrotic and viable tumor with high specificity. The specific augmented accumulation of PpIX and ferritin clusters in metabolically active glioma cells after "ALA plus iron", as demonstrated in FI and prussian blue stating, could guarantee specificity of this method with regards to discrimination of necrosis and metabolically active parts of GBM. Therefore, the suggested method would be of further clinical interest to directly assess accurate auto-segmentation of the tumor volume in radiotherapy in a future study.

However, one of the limitations of this study is intra-tumoral hemorrhage as an interfering factor for ferritin accumulation induced by "ALA plus iron", needs more investigations in future studies. To resolve this problem, performing the subtraction of images before and after "ALA plus iron" might be an effective strategy. Also, iron supplements used in this study can be considered safe in iron-deficient states that are dominant in patients with brain tumor. However, there is only one contraindication in a rare genetic disorder [48,49], which should be considered. Moreover, ALA with a dosage of 20 mg/kg is an FDA-approved organic safe agent used in this study.

5. Conclusion

Our study suggests that ferritin imaging using "ALA + iron supplement" as a metabolic imaging method could discriminate the necrosis and active volume of the tumor, reliably. Therefore, the suggested method could be used for accurate auto-segmentation of the tumor volume in the radiotherapy.

Ethical approval

All ethical approvals required for animal procedures were obtained by the local ethics committee of the National Institute for

Medical Research Development (NIMAD, ethical code: IR. NIMAD.REC.1397.424).

Data availability statement

Data will be made available on request.

CRediT authorship contribution statement

Anita Ebrahimpour: Writing – review & editing, Supervision, Project administration. **Mehdi Khoobi:** Funding acquisition, Conceptualization. **Nader Riyahi Alam:** Validation, Investigation. **Mahboubeh Masoumbeigi:** Writing – original draft, Methodology, Formal analysis. **Fatemeh Tirgar:** Investigation, Data curation. **Tayyebeh Ebrahimi:** Resources, Data curation.

Declaration of competing interest

The authors declare that they have no known competing financial interests or personal relationships that could have appeared to influence the work reported in this paper.

Acknowledgments

The authors appreciate the financial support and assistance of the Tehran University of Medical Sciences (TUMS), and the National Institute for Medical Research Development (NIMAD). The authors as well appreciate the National Brain Mapping Lab (NBML) and TUMS Pre-Clinical Core Facilities (TPCF) for providing magnetic resonance and fluorescence imaging services.

Appendix A. Supplementary data

Supplementary data to this article can be found online at https://doi.org/10.1016/j.heliyon.2024.e28355.

References

[1] S. Shirvalilou, S. Khoei, S. Khoee, In vivo 3T magnetic resonance imaging (MRI) of rat brain glioma-bearing tumor: a comparison with digital caliper measurement and histology, Front. Biomed. Technol. 6 (2) (2019) 73–78.
[2] G.P. Mazzara, et al., Brain tumor target volume determination for radiation treatment planning through automated MRI segmentation, Int. J. Radiat. Oncol. Biol. Phys. 59 (1) (2004) 300–312.
[3] P. Robert, et al., Contrast-to-dose relationship of gadopiclenol, an MRI macrocyclic gadolinium-based contrast agent, compared with gadoterate, gadobenate, and gadobutrol in a rat brain tumor model, Radiology 294 (1) (2020) 117–126.
[4] T. Kanda, et al., Gadolinium-based contrast agent accumulates in the brain even in subjects without severe renal dysfunction: evaluation of autopsy brain specimens with inductively coupled plasma mass spectroscopy, Radiology 276 (1) (2015) 228–232.
[5] P. Marckmann, et al., Nephrogenic systemic fibrosis: suspected causative role of gadodiamide used for contrast-enhanced magnetic resonance imaging, J. Am. Soc. Nephrol. 17 (9) (2006) 2359–2362.
[6] R. Manon, et al., The impact of mid-treatment MRI on defining boost volumes in the radiation treatment of glioblastoma multiforme, Technol. Cancer Res. Treat. 3 (3) (2004) 303–307.
[7] A. Pirzkall, et al., MR-spectroscopy guided target delineation for high-grade gliomas, Int. J. Radiat. Oncol. Biol. Phys. 50 (4) (2001) 915–928.
[8] S.J. Nelson, Multivoxel magnetic resonance spectroscopy of brain Tumors 1, Mol. Cancer Therapeut. 2 (5) (2003) 497–507.
[9] S. Marbacher, et al., Use of fluorescence to guide resection or biopsy of primary brain tumors and brain metastases, Neurosurg. Focus 36 (2) (2014) E10.
[10] J. Yamamoto, et al., 5-Aminolevulinic acid: pitfalls of fluorescence-guided resection for malignant gliomas and application for malignant glioma therapy, J. UOEH 42 (1) (2020) 27–34.
[11] S. Kaneko, S. Kaneko, Fluorescence-guided resection of malignant glioma with 5-ALA, Int. J. Biomed. Imag. (2016) 2016.
[12] H.R. Cho, et al., Malignant glioma: MR imaging by using 5-aminolevulinic acid in an animal model, Radiology 272 (3) (2014) 720–730.
[13] A. Ebrahimpour, et al., Detection of glioblastoma multiforme using quantitative molecular magnetic resonance imaging based on 5-aminolevulinic acid: in vitro and in vivo studies, Magn. Reson. Mater. Phys., Biol. Med. (2021) 1–13.
[14] A. Ebrahimpour, et al., Detection of glioblastoma multiforme using quantitative molecular magnetic resonance imaging based on 5-aminolevulinic acid: in vitro and in vivo studies, Magn. Reson. Mater. Phys., Biol. Med. 35 (1) (2022) 3–15.
[15] S. Hingtgen, et al., Real-time multi-modality imaging of glioblastoma tumor resection and recurrence, J. Neuro-oncol. 111 (2013) 153–161.
[16] S. Linsler, et al., Fluorescence image-guided resection of intracranial meningioma: an experimental in vivo study on nude mice, Ann. Anatom.-Anatom. Anzeig. 237 (2021) 151752.
[17] K.S. Samkoe, et al., Protoporphyrin IX fluorescence contrast in invasive glioblastomas is linearly correlated with Gd enhanced magnetic resonance image contrast but has higher diagnostic accuracy, J. Biomed. Opt. 16 (9) (2011), 096008-096008-7.
[18] A. Ebrahimpour, N. Riahi Alam, M. Khoobi, The potential of 5-aminolevulinic acid as a contrast agent in MR imaging: challenges and opportunities, J. Sci. Islam. Repub. Iran 32 (1) (2021) 15–28.
[19] H.W. de Haan, Mechanisms of proton spin dephasing in a system of magnetic particles, Magn. Reson. Med. 66 (6) (2011) 1748–1758.
[20] T. Li, A. Aisen, T. Hindmarsh, Assessment of hepatic iron content using magnetic resonance imaging, Acta Radiol. 45 (2) (2004) 119–129.
[21] D.A. Yablonskiy, et al., In vivo evaluation of heme and non-heme iron content and neuronal density in human basal ganglia, Neuroimage 235 (2021) 118012.
[22] Y. Wang, Quantitative susceptibility mapping: magnetic resonance imaging of tissue magnetism, CreateSpace (2013).
[23] Y. Wang, et al., Clinical quantitative susceptibility mapping (QSM): biometal imaging and its emerging roles in patient care, J. Magn. Reson. Imag. 46 (4) (2017) 951–971.